

Article

Digital twin technology in biomechanics: Revolutionizing human movement analysis and rehabilitation practices

Jiaqi Yang¹, Muxin Luo¹, Weijia Zhi², Xuefeng Liu^{3,*}¹ Sun Yueqi College, China University of Mining and Technology, Xuzhou 221116, China² School of Economics and Management, China University of Mining and Technology, Xuzhou 221116, China³ School of Public Management, China University of Mining and Technology, Xuzhou 221116, China* **Corresponding author:** Xuefeng Liu, liuxuefeng@cumt.edu.cn

CITATION

Yang J, Luo M, Zhi W, Liu X.
Digital twin technology in
biomechanics: Revolutionizing
human movement analysis and
rehabilitation practices. *Molecular &
Cellular Biomechanics*. 2025; 22(4):
1288.
<https://doi.org/10.62617/mcb1288>

ARTICLE INFO

Received: 2 January 2025

Accepted: 17 January 2025

Available online: 7 March 2025

COPYRIGHT



Copyright © 2025 by author(s).
Molecular & Cellular Biomechanics
is published by Sin-Chn Scientific
Press Pte. Ltd. This work is licensed
under the Creative Commons
Attribution (CC BY) license.
[https://creativecommons.org/licenses/
by/4.0/](https://creativecommons.org/licenses/by/4.0/)

Abstract: Lower limb rehabilitation exoskeletons are wearable assistive rehabilitation devices designed to protect and aid patients in rehabilitation training. However, traditional lower limb rehabilitation exoskeleton systems are limited by information acquisition technology, mostly adopting passive training with fixed trajectories and lacking real-time motion data interaction, resulting in deficiencies in the overall system's safety and autonomy. Based on this, this study proposes a lower limb rehabilitation exoskeleton system based on digital twin technology. By leveraging digital twin technology, the system achieves a deep integration of virtual and physical spaces, improves human-machine information interaction technology, and enhances the effectiveness of rehabilitation training. Experimental results demonstrate that the system can achieve personalized gait trajectory planning and real-time motion data interaction, providing a new solution for lower limb rehabilitation.

Keywords: lower limb exoskeleton; digital twin; virtual simulation; gait planning

1. Introduction

With the increasing aging of the population, the number of patients with physical movement disorders caused by cerebrovascular diseases shows an increasing trend year by year. As a more common limb movement disorder, the lower limb movement disorder needs to be combined with scientific rehabilitation training to recover, so that the patient can restore the lower limb walking ability [1]. The lower limb exoskeleton robot is a mechanical and electrical equipment that wears the human lower limbs and cooperates with the lower limbs. It can simulate the patient's limb movement track, assist the patient to carry out lower limb training, and then realize the rehabilitation treatment of the patient's lower limbs. However, due to the different human gait, it is difficult to ensure the effective rehabilitation of patients with various pathologies, and there are certain safety risks [2]. With people's attention, many scholars have carried out research on gait planning. Some studies have proposed a gait planning scheme based on linkage model and zero point moment, which can realize the adaptive walking of exoskeleton on different ground [3]. Some studies have proposed a gait planning scheme based on artificial intelligence algorithm, which mainly takes human gait parameters as input and gait trajectory as output, and constructs a training neural network, so as to obtain the stable motor gait trajectory of human exoskeleton [4]. In other studies, the fuzzy controller was used to adjust the joint angle and torque according to the real-time state parameters, and then to plan the stable gait trajectory of the exoskeleton.

However, the development cost of this method is relatively large [5]. Digital twin technology, as a cutting-edge digital technology.

On the basis of information perception and real-time communication, the expression entity is constructed in the virtual space in the form of digitalization, and the virtual body is simulated, so as to achieve the purpose of controlling the entity and realize the two-way dynamic mapping of the virtual body and the entity bond. In the field of rehabilitation robot application, some studies have proposed a rehabilitation equipment design method that considers the clinical environment factors based on the concept of digital twin. The model establishment and the production of rehabilitation equipment can reduce the time and cost of rehabilitation equipment development [6]. To alleviate the lack of interaction between patients and rehabilitation equipment, a study designed an automatic gait data control system for digital twin, the sensor obtained gait information sent to the computer software for patient gait analysis, the effectiveness and real-time performance of human-computer interaction is improved, can realize the data interaction between robot and patient [7]. However, existing studies consider relatively little about safety and focus only on development time and cost.

Based on this, this paper takes the lower limb rehabilitation exoskeleton as the research object and constructs a digital twin system for lower limb rehabilitation exoskeletons based on digital twin technology. Through the real-time mapping of physical devices by digital twin technology, trajectories are planned in real-time according to the patient's movement needs and posture. Additionally, the digital twin system monitors the real-time motion status of the lower limb exoskeleton and the wearer, providing timely feedback and optimization, verifying the safety of equipment use, and ensuring effective rehabilitation and safety for the wearer.

2. Design of personalized gait planning and digital twin system for lower limb rehabilitation exoskeletons

2.1. Personalized gait planning for lower limb rehabilitation exoskeletons

2.1.1. Analysis of gait parameters of human lower limbs

Human walking is a cyclic action involving alternating and repetitive changes in the position of the lower limbs. The kinematic relationship of the human lower limbs is illustrated in **Figure 1**.

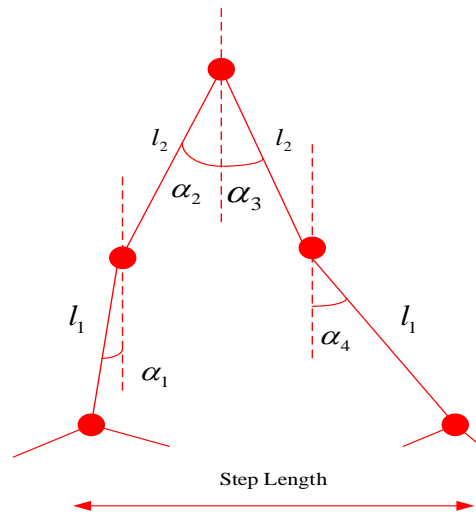


Figure 1. Kinematic relationship of human lower limbs.

As can be seen from **Figure 1**, there exists the following relationship between step length and lower limb joints as well as joint angles:

$$Steplength = l_1(\sin \alpha_1 + \sin \alpha_3) + l_2(\sin \alpha_2 + \sin \alpha_4) \quad (1)$$

In Equation (1), α_1 and α_3 , as well as α_2 and α_4 , represent adjacent gaits of the left and right legs, differing by half a gait cycle. From this, it can be inferred that the step length of the human body is related to the length of the lower limbs and the joint movement angles. Due to the corresponding differences in human lower limbs, the study calculates the lengths of various segments of the lower limbs for different body types based on the Chinese standard B/T17245-2004 “Anthropometric Parameters of Adults” [7].

Assuming L_1 , L_2 , and L_3 represent the lengths of the thigh, calf, and foot respectively, and X_1 and X_2 represent body weight and height, we have:

$$\begin{cases} L_1 = (-122.52 - 0.13X_1 + 0.235X_2)/0.547 \\ L_2 = (23.47 - 0.5X_1 + 0.095X_2)/0.607 \\ L_3 = (35.13 - 0.02X_1 + 0.03X_2)/0.514 \end{cases} \quad (2)$$

Based on the Asian anthropometric standards and research analysis of various parts of the human lower limbs, the average dimensions and lengths of various segments of the lower limbs of healthy Asian adults are presented in **Table 1**.

Table 1. Dimensions and lengths of lower limbs for adult males/females (unit: mm).

| Lower Limb Segments: | Gender | Maximum Value | Minimum Value | Average Value |
|----------------------|--------|---------------|---------------|---------------|
| Thigh | Male | 507.59 | 425.89 | 455.88 |
| | Female | 475.88 | 431.66 | 453.65 |
| Calf | Male | 405.45 | 335.45 | 369.88 |
| | Female | 339.88 | 303.55 | 317.65 |
| Foot | Male | 77.69 | 66.78 | 69.88 |
| | Female | 64.56 | 57.98 | 61.56 |

Based on the data information in **Table 1**, the individual segment lengths of the lower limbs corresponding to different body types can be obtained through Equation (2). Furthermore, after determining the lower limb dimensions using Equation (1), gait trajectory planning can be achieved [8].

2.1.2. Gait data acquisition

Selection of data acquisition equipment

In this study, optical capture equipment was primarily used to collect motion data of the human lower limb joints, in order to obtain actual joint gait trajectories [8]. During the experiment, the subjects were required to maintain their hands above their chest to ensure the accuracy of the experiment. For each trial, the three-dimensional coordinate data of the reflective markers on the subjects' lower limbs within a 20-s period within the capture area were recorded. The aim was to more accurately capture and analyze the lower limb motion trajectories and posture changes of the subjects during walking.

Research subjects

In this study, 30 physically healthy young adults, all aged 24 years and with a gender ratio of 1:1, were selected as test subjects.

Experiment 1: One healthy youth with a height of 175 cm was chosen to walk on a treadmill at speeds of 1.0 km/h, 2.0 km/h, 3.0 km/h, 4.0 km/h, and 5.0 km/h.

Experiment 2: Five healthy youths with heights of 185 cm, 180 cm, 175 cm, 170 cm, and 165 cm, respectively, were selected to walk on a treadmill at a constant speed of 3.0 km/h.

Experiment 3: One adolescent was chosen to perform squats, climb a slope, and navigate stairs within the designated test area, with these actions being recorded.

Spatial coordinate data of the reflective markers were recorded separately for each experiment within a duration of 60 s [9].

To effectively enhance the accuracy of experimental data, test subjects are required to wear tight-fitting clothing during the testing process and have six reflective markers attached to their lower limbs, specifically at the waist (labeled as *B1*), hip joint (*B2*), thigh (*B3*), knee joint (*B4*), calf (*B5*), and ankle joint (*B6*). After the placement of these markers, infrared capture cameras are utilized to capture the positions of each marker, which are then input into specialized software for identification. This process is employed to create the linkage (Link) for the lower limb segments.

To achieve gait planning within a cycle, the study selected joint angle variations from one gait cycle and analyzed the processed actual gait trajectories. The results are shown in **Figures 2** and **3**.

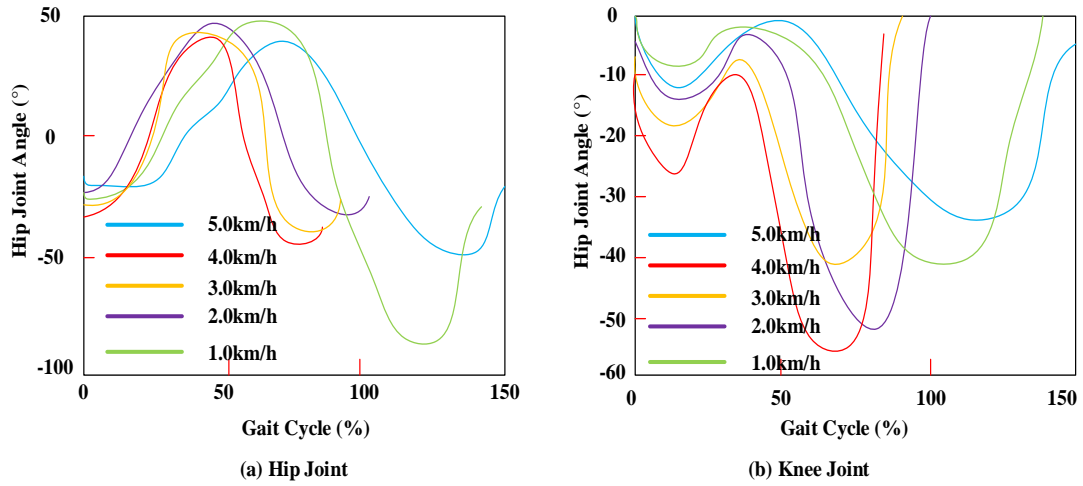


Figure 2. Joint angle trajectories at different speeds: **(a)** Hip Joint; **(b)** Knee Joint.

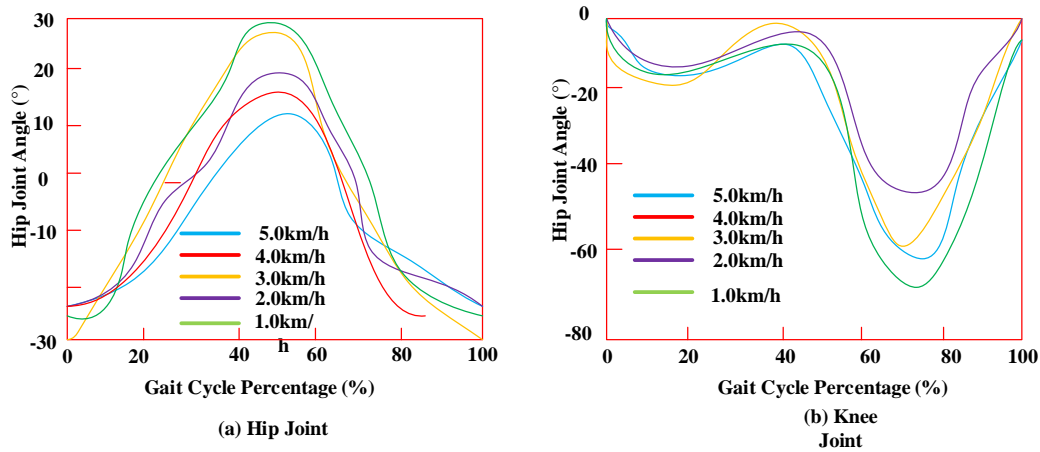


Figure 3. Joint angle trajectories at the same speed: **(a)** Hip Joint; **(b)** Knee Joint.

As clearly shown in **Figures 2** and **3**, under the conditions of different speeds and body types, the step length and gait cycle of the gait trajectories undergo corresponding changes. By fitting these characteristic parameters, the corresponding gait trajectories can be obtained [10].

2.1.3. Construction of a personalized gait planning model for lower limbs

Extraction of characteristic parameters from gait trajectory

In this research process, the Bernstein equation was employed to fit the joint trajectory curves obtained from Experiment 2, in order to obtain the characteristic parameters of the joint curves, namely:

$$L(t; \lambda_j, \omega) = \sum_{j=0}^n P_j b_{j,n}(t) \quad (3)$$

In Equation (3), t represents the gait cycle, and $t \in [0,1]$; P_j denotes a set of given control points, and $P_j \in R^u (u = 2,3; j = 0,1, \dots, n)$; $b_{j,n}(t)$ is the basis function for the n gait motion curve; ω stands for the overall control parameter, and $\omega \in [0,1]$; λ_j represents the shape control parameter, and it has:

$$0 \leq \lambda_j \leq \binom{n}{j} (j = 0, 1, \dots, n), \binom{n}{j} = \frac{n!}{j!(n-j)!} \quad (4)$$

After completing the curve fitting, the average gait curves of the hip and knee joints are converted into scatter plot form and substituted into Equation (5) to obtain the overall common control points of the curves.

$$(P_1, P_2, \dots, P_n) \begin{pmatrix} b_{0,n}(t) \\ b_{1,n}(t) \\ \vdots \\ b_{n,n}(t) \end{pmatrix} = (l_1, l_2, \dots, l_n) \quad (5)$$

In Equation (5), P_1, P_2, \dots, P_n represents the common control points, and l_1, l_2, \dots, l_n represents the discrete points.

At this point, by fitting the gait trajectory curves of young individuals with different body types using Equation (5), the corresponding shape control parameters λ_j for the curves can be obtained, as detailed in **Table 2**.

Table 2. Shape control parameters λ_j for hip joints of young individuals with different body types.

| Body posture and height (cm) | | Average shape control parameters | | | | | |
|------------------------------|------------|----------------------------------|-------------|-------------|-------------|-------------|-------------|
| | | λ_1 | λ_2 | λ_3 | λ_4 | λ_5 | λ_6 |
| 185 | Hip Joint | 5.68 | 13.19 | 24.19 | 14.08 | 5.68 | 2.48 |
| | Knee Joint | 4.88 | 17.88 | 21.58 | 24.06 | 4.88 | 5.55 |
| 180 | Hip Joint | 5.19 | 11.68 | 18.47 | 19.55 | 5.19 | 2.78 |
| | Knee Joint | 8.26 | 9.45 | 21.18 | 24.24 | 8.26 | 2.68 |
| 175 | Hip Joint | 5.18 | 11.68 | 18.60 | 19.60 | 5.18 | 2.78 |
| | Knee Joint | 4.98 | 7.10 | 24.30 | 17.20 | 4.98 | 4.88 |
| 170 | Hip Joint | 4.09 | 13.88 | 15.18 | 22.27 | 4.09 | 3.19 |
| | Knee Joint | 3.28 | 14.09 | 22.48 | 27.87 | 3.28 | 2.68 |
| 165 | Hip Joint | 3.65 | 13.18 | 13.19 | 18.09 | 9.90 | 4.19 |
| | Knee Joint | 1.09 | 9.70 | 14.88 | 13.10 | 10.40 | 3.08 |

Similarly, by fitting different trajectory curves at various speeds using Equation (5), the obtained shape control parameters are shown in **Table 3**.

Table 3. Shape control parameters λ_j for hip joints at different speeds.

| Speed (km/h) | | Mean Shape Control Parameters | | | | | |
|--------------|------------|-------------------------------|-------------|-------------|-------------|-------------|-------------|
| | | λ_1 | λ_2 | λ_3 | λ_4 | λ_5 | λ_6 |
| 5.0 | Hip Joint | 8.19 | 15.28 | 18.70 | 29.38 | 8.49 | 1.29 |
| | Knee Joint | 10.88 | 13.88 | 21.29 | 26.17 | 7.29 | 4.18 |
| 4.0 | Hip Joint | 6.77 | 14.68 | 18.80 | 24.30 | 9.68 | 2.48 |
| | Knee Joint | 5.18 | 14.48 | 19.19 | 22.29 | 5.55 | 3.68 |
| 3.0 | Hip Joint | 4.68 | 14.47 | 15.90 | 26.18 | 10.88 | 4.77 |
| | Knee Joint | 3.68 | 8.09 | 17.30 | 16.55 | 6.35 | 3.84 |

Table 3. (Continued).

| Speed (km/h) | | Mean Shape Control Parameters | | | | | |
|--------------|------------|-------------------------------|-------------|-------------|-------------|-------------|-------------|
| | | λ_1 | λ_2 | λ_3 | λ_4 | λ_5 | λ_6 |
| 2.0 | Hip Joint | 3.48 | 12.68 | 15.70 | 24.18 | 13.36 | 6.65 |
| | Knee Joint | 4.09 | 11.68 | 18.47 | 22.29 | 9.18 | 4.77 |
| 1.0 | Hip Joint | 2.88 | 8.78 | 14.55 | 23.48 | 15.78 | 8.85 |
| | Knee Joint | 1.27 | 13.85 | 23.89 | 11.87 | 7.28 | 4.78 |

Using the data in **Tables 1** and **2** as the characteristic parameters of the joint curves, and taking human body shape characteristics and desired walking speed as inputs, a gait parameter model is constructed to output the characteristic parameters of the joint curves, thereby obtaining the gait trajectories of the lower limbs [11].

Motion scenario model and gait parameter model

In lower limb gait rehabilitation, the involved motion scenarios exhibit corresponding differences, resulting in varied lower limb gait trajectories. To address this, the study employs Optical Capture Experiment 3 to obtain trajectories for three corresponding motion scenarios, as shown in **Figure 4**. The coordinates of the common control points of the joints for the corresponding scenarios are detailed in **Table 4**.

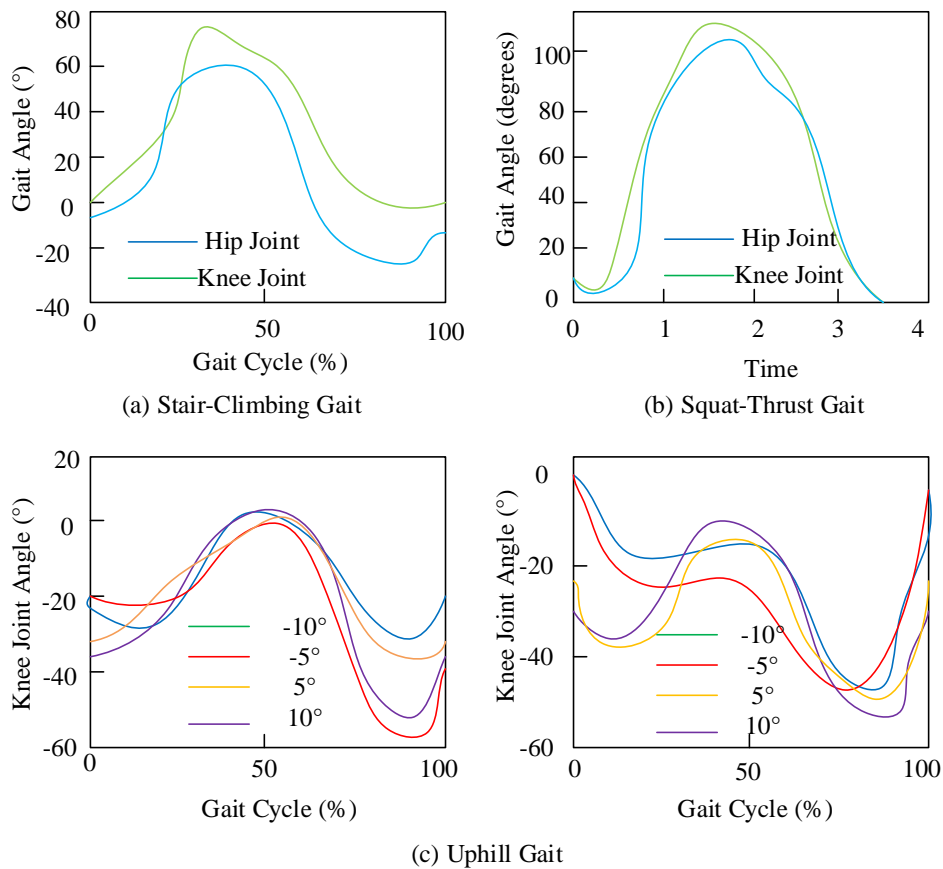


Figure 4. Actual joint trajectories of the human body in different motion scenarios: **(a)** Stair-Climbing Gait; **(b)** Squat-Thrust Gait; **(c)** Uphill Gait.

Among them, **Figure 4a** shows the gait track of the same teenager in climbing stairs, **Figure 4b** shows the gait track of squatting action, and **Figure 4c** shows the gait track of climbing with different slopes.

In this study, we utilize the motion scenario model and its related conditional parameters as input to calculate the coordinates of the common control points of the joint curves, thereby determining the overall trend of the joint curves [12]. By applying Equation (5) to fit and analyze the gait curves under three different motion scenarios, we obtain the common control points for the corresponding scenario trajectories, as detailed in **Table 4**.

Table 4. Coordinates of common control points of joints for corresponding scenarios.

| Motion Scenario | Climbing stairs | | Climbing slopes | | Squatting down | |
|-----------------|-----------------|---------------|-----------------|---------------|----------------|-------------|
| | Hip Joint | Knee Joint | Hip Joint | Knee Joint | Hip Joint | Knee Joint |
| Joint | | | | | | |
| B1 | 0, 0.20 | 0, 1.60 | 0, -31.38 | 0, -27.19 | 0, 5.68 | 0, 0.80 |
| B2 | 29, -5.80 | 21, 0.60 | 23, -44.78 | 7, -51.37 | 1.09, 39.77 | 1.19, 40.3 |
| B3 | 33, 60.80 | 33, 54.68 | 31.48, -7.78 | 22, -49.68 | 2.48, 124.48 | 2.1, 140.68 |
| B4 | 55.39, 43.49 | 37.48, 102.66 | 51.49, 25.00 | 45, -10.48 | 3.58, 18.33 | 2.5, 25.78 |
| B5 | 71, -50.68 | 51.48, 60.68 | 71, -18.09 | 78.49, -69.01 | 3.5, 1.90 | 3.5, 1.90 |
| B6 | 95.58, -20.38 | 72.79, -2.60 | 90, -41.68 | 82.01, -75.55 | | |

The experimental results demonstrate the mapping relationship between different motion scenarios and the corresponding common control points of joint curves. Based on this dataset, a gait parameter trajectory prediction model based on a neural network is constructed, as shown in **Figure 5**. The model consists of two input nodes (receiving motion scenarios and their conditional parameters respectively), one output layer with 14 output nodes (representing the common control points of hip and knee joints), and a hidden layer with 24 neurons. The neural network model is trained using the BP (backpropagation) algorithm. This motion scenario model can instantly output the common control points of the corresponding gait trajectory based on the input scenario and its conditional parameters, thereby capturing the overall trend of the gait trajectory in that motion scenario through these control points [13].

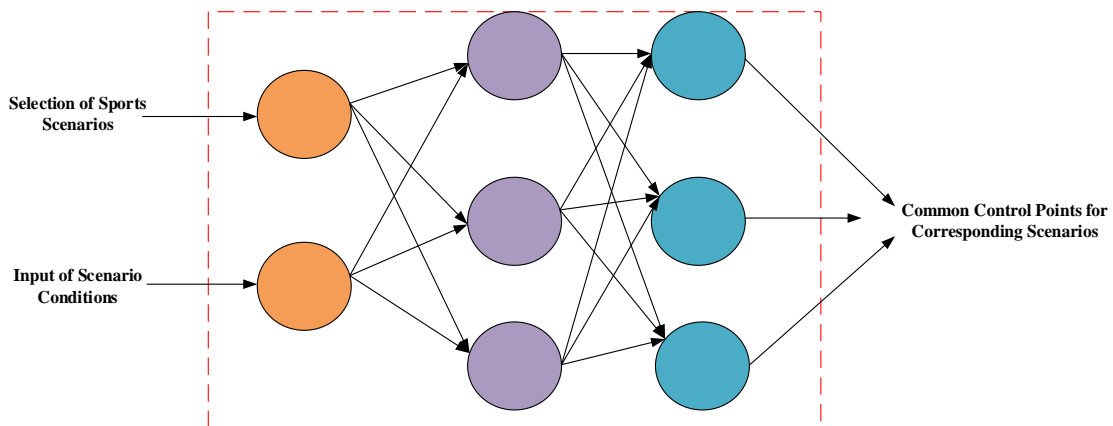


Figure 5. Motion scenario model.

For the gait parameter model, its construction method is similar to that of the motion scenario model, primarily using human body parameters and desired walking speed to predict joint trajectories and, based on shape control parameters, to predict gait trajectory parameters [14]. By making corresponding changes to these parameters, different gait trajectories can be obtained, thereby constructing a gait parameter trajectory model, as shown in **Figure 6**.

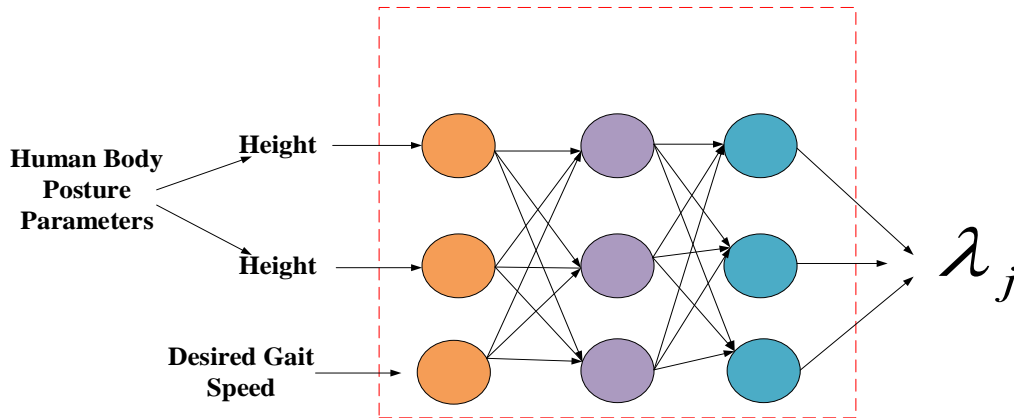


Figure 6. Gait parameter model.

After inputting the human body posture parameters and desired gait speed, the gait parameter model outputs shape control parameters that govern the local shape of the trajectory. By fitting Equation (5), the angle change curves of each joint are obtained, thereby enabling personalized lower limb gait trajectory planning.

2.2. Design of a digital twin system for lower limb rehabilitation exoskeletons

2.2.1. System composition

The geometric structure model focuses on depicting the geometric shape, dimensions, and dynamic connections between components of the exoskeleton prototype; the physical mechanics model conducts in-depth analysis of stress distribution patterns and the moments borne by joints under various motion scenarios for the exoskeleton; the behavioral response model aims to make immediate adjustments based on any changes in the skeletal state; the agent interaction model specializes in processing and responding to any changes in exoskeleton joint angles; finally, the safety rule evaluation model is responsible for comprehensively evaluating all motion parameters to ensure they comply with established safety standards [15].

2.2.2. Design and development of the digital twin system platform

Setup of the system development environment

Utilizing Unity and Python technologies, this paper designs and implements a digital twin system equipped with a user interface. The system architecture is divided into two parts: The client and the backend data. The backend data component encompasses gait function service modules, real-time data exchange modules, and a historical data storage database. The client part is developed based on the PyQt5

framework, with core functions including virtual simulation demonstrations of twin models, real-time monitoring of exoskeleton prototype status, and online planning of gait paths. The specific technical environment configuration for system development is detailed in **Table 5**.

Table 5. System development environment.

| Project | Hardware/Software |
|----------------------------|--------------------------|
| Operating System | Win10 |
| Basic Development Platform | Unity 2019 |
| IDE | VS, MATLAB, PyCharm |
| Programming Language | C#, Python |
| Communication Method | Socket, OPC UA |

Integrated design of data backend

The crucial role of the data backend lies in facilitating data circulation and integration of model algorithms between systems. The digital twin system for lower limb exoskeletons achieves precise correspondence between the virtual and physical environments through data interaction between its twin model and the physical exoskeleton. To ensure timely data transmission and updates, we have carefully constructed a data communication service system that serves as the hub connecting and coordinating the various modules of the system [16]. Its comprehensive functionality not only covers real-time data capture and storage but also enables bidirectional communication between the virtual and physical worlds, allowing the human-computer interaction interface to reflect changes in the status of both the physical exoskeleton and the digital twin model in real-time. In constructing the algorithms for the digital twin model, we integrated the predictive analysis capabilities of the safety assessment model with multi-objective optimization algorithms for gait trajectories. The safety assessment model is further decomposed into an agent-based stress prediction module, a dynamics-based joint torque prediction module, and a stability assessment module based on ZMP (Zero Moment Point, zero torque point). After successfully integrating these algorithm modules into the system, we reiterate the importance of the data communication service [17]. It is not only critical for real-time data transmission and updates within the system but also ensures immediate data capture, storage, and seamless communication between the virtual and physical worlds, providing a solid foundation for the stable operation of the system.

Integrated development of client-side applications

The client-side application is built on the PyQt5 framework, integrating all visual elements into a unified Qt interface. For the digital twin system of lower limb rehabilitation exoskeletons, the human-computer interaction interface is meticulously divided into three main modules based on its functional characteristics: Real-time status monitoring, interactive control between the physical and virtual exoskeletons, and customized gait planning services [18]. The real-time status monitoring module dynamically displays angle data of each joint during movement in the form of graphs on the interface through the system's internal real-time data circulation mechanism,

providing users with intuitive visual feedback. Additionally, this module integrates camera monitoring functionality and the twin model from the Unity operation interface, enabling users to observe every detail of the movement status in real-time. The interactive control module between the physical and virtual exoskeletons provides users with the ability to control both the physical exoskeleton and its digital twin simultaneously through the human-computer interaction interface. Users can not only drive the movement of the physical exoskeleton by manipulating the twin model but also receive real-time feedback on the movement status of the physical exoskeleton from the twin model, achieving seamless interaction between the virtual and real worlds. The customized gait planning services module focuses on meeting users' personalized adjustment needs for movement scenarios and requirements [19]. Users can select a suitable scenario from four preset movement scenarios and input the patient's physical characteristics and desired movement speed. Subsequently, the system employs advanced personalized gait planning technology to generate an initial optimized movement trajectory for the user. On this basis, the system further utilizes multidisciplinary optimization algorithms based on the exoskeleton digital twin model for multiple iterative simulations to ensure that the final generated gait trajectory not only meets users' expectations but also achieves optimal movement effects [20].

3. System testing

3.1. Establishing an experimental platform

After the exoskeleton is worn by the human body, the lower limbs of the human body will be tightly combined with it. If sensors are placed on the medial side of the lower limbs, it will seriously affect the movement of the wearer's lower limbs. Therefore, they need to be placed on the lateral side. The driving equipment of the exoskeleton prototype is Siemens S7-1500, which establishes communication with the human-computer interaction interface through OPC UA to drive the movement of the exoskeleton [21].

3.2. System function testing

3.2.1. Virtual control via real-time data testing

During this research process, sensors installed on the exoskeleton prototype were used to collect changes in joint angles and compare them with feedback information from the model's moving joints. The results are shown in **Figure 7**.

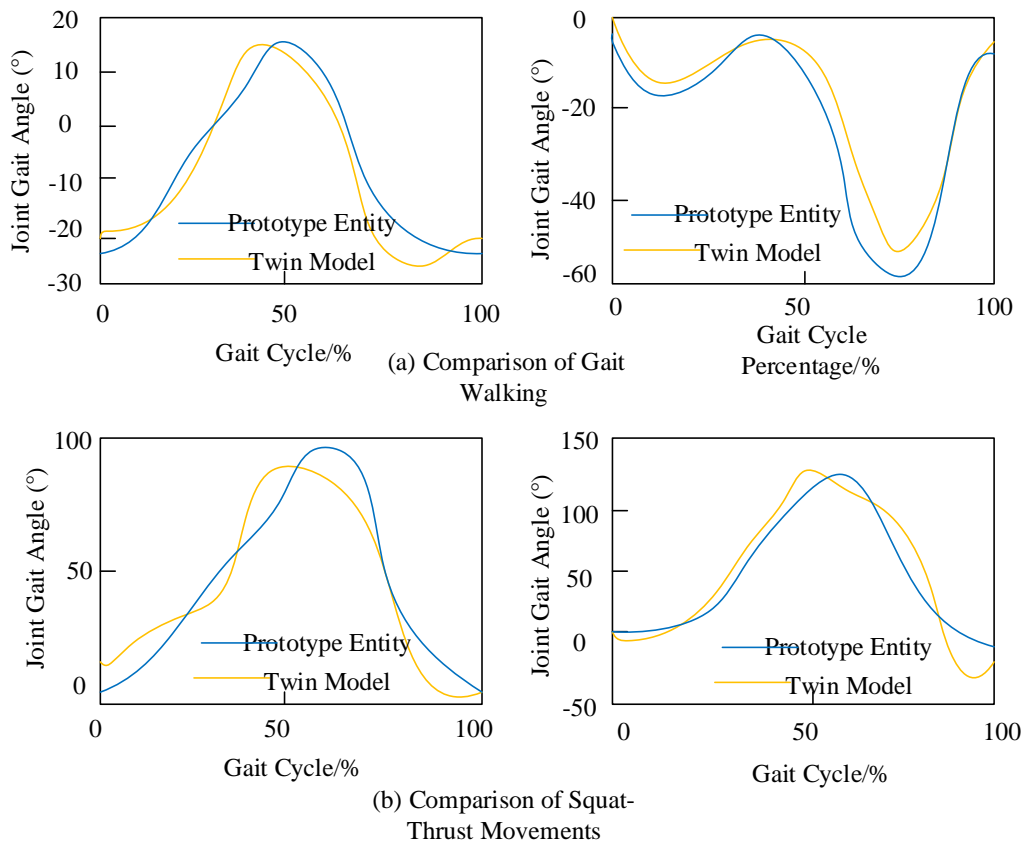


Figure 7. Trajectory comparison between Twin model and prototype: **(a)** Comparison of Gait Walking; **(b)** Comparison of Squat-Thrust Movements.

As shown in **Figure 7**, under two different motion scenarios, the average errors of the trajectories are 3.09° and 2.31° , respectively. This indicates that the motion of the twin model can fully reflect the motion posture of the exoskeleton prototype, enabling real-time monitoring of the motion state [22].

3.2.2. Virtual-to-real control experiment

Using the normal walking gait trajectory at 3.0 km/h as input, the comparison of the motion paths output by the exoskeleton prototype and the digital twin model is shown in **Figure 8**.

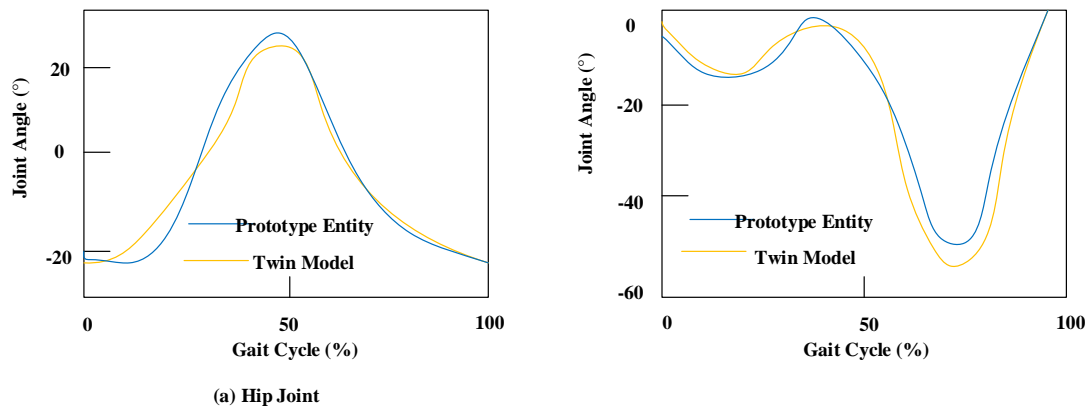


Figure 8. Comparison of control trajectory effects between prototype entity and Twin model: **(a)** Hip Joint; **(b)** Gait Cycle.

As clearly shown in **Figure 8**, the average error of the system-output trajectory is 1.72° , indicating that with the feedback from the twin model, the exoskeleton prototype can accurately perform the corresponding gait trajectory. Although there is a corresponding error, it is relatively small.

3.2.3. Online gait planning test for exoskeleton

After setting up the experimental environment, detailed gait planning was conducted for four specific motion scenarios: Normal walking (at a speed of 3.0 km/h), squatting and standing up (with a maximum squatting angle of 120°), climbing a slope (at an angle of 10° and a speed of 3.0 km/h), and ascending stairs (with each step being 15 cm high). Operators can input corresponding parameters and desired speeds on the human-computer interaction interface based on the selected motion scenario. Subsequently, the system plans the target motion trajectory based on these inputs, combined with the motion scenario and gait parameter model, and imports it into the digital twin model of the exoskeleton for virtual simulation experiments [23]. In this process, we utilized an improved genetic algorithm to further optimize the target trajectory.

For each experimental action, three repeated measurements were conducted, with each gait lasting 10 s. Since attitude sensors may be interfered with by external factors during data acquisition, leading to data instability, necessary preprocessing was performed on the collected data. Subsequently, the actual motion trajectory of the exoskeleton prototype was measured through the experimental platform. During the testing process, it was found that the optimized trajectory could guide the exoskeleton prototype to move more accurately along the target trajectory, with relatively small deviations between them. However, some errors still existed, mainly due to the hardware assembly of the exoskeleton prototype, especially during the assembly of hip and knee joints, where actual joint clearances resulted in certain deviations from the target trajectory during actual measurements [24].

To this end, Equations (6) were employed to calculate the mean error *MAE* and mean percentage error *MAPE* of the exoskeleton's motion. The calculation results are detailed in **Table 6**.

$$\begin{cases} MAE = \frac{1}{n} \sum_{i=1}^n |p_i - r_i| \\ MAPE = \frac{100\%}{n} \sum_{i=1}^n \left| \frac{p_i - r_i}{r} \right| \end{cases} \quad (6)$$

In Equation (6), n represents the number of sampling times; r_i denotes the target trajectory under the i -th sampling; and p_i represents the gait angle of the actual motion trajectory under the i -th sampling.

Table 6. Joint angle errors for different motion scenarios (unit: Degrees).

| Different gait joints | MAE | MAPE |
|---|------|------|
| Hip joint during walking | 0.86 | 0.35 |
| Knee joint during walking | 1.54 | 0.31 |
| Hip joint during squatting and standing up | 3.28 | 1.77 |
| Knee joint during squatting and standing up | 4.19 | 2.88 |
| Hip joint during climbing uphill | 1.71 | 0.78 |
| Knee joint during climbing uphill | 1.88 | 1.47 |
| Hip joint during climbing stairs | 4.69 | 3.44 |
| Hip joint during climbing stairs | 5.81 | 3.91 |

Through analysis of **Table 6**, it is evident that the personalized planning of the digital twin system performs well in walking and uphill climbing scenarios, with relatively small errors. Although the accuracy of gait for squatting and standing up, as well as stair climbing, is lower, the errors remain small, indicating that the online gait planning function of the digital twin system has a relatively high degree of accuracy [25].

3.3. Exoskeleton gait planning test

During this research process, the traditional PID (Proportional Integral Differential) algorithm and the digital twin algorithm were utilized to optimize the exoskeleton gait, and the optimization effects of the two algorithms were compared. The details are shown in **Table 7**.

Table 7. Comparison of exoskeleton gait optimization effects.

| Optimization Algorithms | Number of Iterations (times) | Time Consumption (seconds) | Average Trajectory Error (degrees) |
|---------------------------|------------------------------|----------------------------|------------------------------------|
| Traditional PID Algorithm | 14 | 6.50 | 5.30 |
| Digital Twin Algorithm | 159 | 5.30 | 1.94 |

Through analysis of **Table 7**, it is found that when the number of iterations is 14, the traditional PID algorithm consumes a time of 6.50 s with an average trajectory error of 5.30 degrees. In contrast, the digital twin algorithm, with a number of iterations of 159, consumes a time of 5.30 s and achieves an average trajectory error of 1.94 degrees. Therefore, it can be concluded that the digital twin algorithm can significantly improve the performance of the exoskeleton prototype, playing a crucial role in rehabilitation training for patients with lower limb impairments.

4. Conclusion

This paper successfully studies and implements a digital twin-based lower limb rehabilitation exoskeleton system, which is significantly innovative and practical in the field of rehabilitation. By constructing a digital twin model of lower limb rehabilitation exoskeleton, we realize the precise planning and optimization of

patients' gait trajectory, which not only improves the pertinence and effectiveness of rehabilitation training, but also provides patients with a more comfortable and personalized rehabilitation experience. The experimental results show that the system can accurately capture and analyze the patient's gait characteristics and generate a personalized gait trajectory according to the patient's posture and motion scene. After several iterations of optimization, the system gradually eliminates the Angle error and improves the accuracy of the gait trajectory, thus ensuring the quality and effect of the rehabilitation training. In addition, the system also has real-time monitoring and feedback functions, which can monitor the movement state of the exoskeleton prototype in real time, and feedback the data to the system for iterative optimization. This virtual-real interaction method not only improves the intelligence level of the system, but also provides more reliable and accurate data support for rehabilitation training. But due to the lack of experimental conditions and time, this paper still has certain limitations, mainly embodied in: First, in view of the lower limb rehabilitation exoskeleton prototype can use digital twin technology to develop other functions, subsequent design can consider the digital twin model of human body, through human body and exoskeleton interaction between virtual human-machine coupling model. Second, the designed digital twin system is only for one exoskeleton device, and the utilization rate of the system is relatively low. The subsequent design can consider the linkage control of multiple exoskeleton devices to improve the use efficiency of the overall system. Looking into the future, we will continue to deeply study the application potential of digital twin technology in the field of rehabilitation, and explore more innovative rehabilitation methods and means. It will further improve the function and performance of the system, improve the accuracy and real-time performance of gait planning, and provide better rehabilitation services for patients.

Author contributions: Conceptualization, JY and XL; methodology, ML; software, JY; validation, JY, WZ and XL; formal analysis, ML; investigation, WZ; resources, XL; data curation, JY; writing—original draft preparation, JY; writing—review and editing, ML and WZ; visualization, JY; supervision, XL; project administration, XL; funding acquisition, XL. All authors have read and agreed to the published version of the manuscript.

Ethical approval: Not applicable.

Funding: CUMT Basic Research Funds (Grant Number: 2023ZDPYSK09); Innovation and Entrepreneurship Training Project for College students of CUMT (Grant Number: 202310290087Z); Humanities and Social Sciences Project of Ministry of Education (Grant Number: 22YJA630043).

Conflict of interest: The authors declare no conflict of interest.

References

1. Guo H, Zhou X, Du Q. Research progress on the improvement of walking ability in children with cerebral palsy using lower limb rehabilitation robots. *China Rehabilitation Medicine*. 2021; 36(6): 6–9.

2. Lei J, Tang J. Current status and application of lower limb rehabilitation robots in improving walking ability for patients with spinal cord injury. *Medical Information*. 2022; 35(19): 159–62.
3. Viteckova S, Kutilek P, De Boisboissel G, et al. Empowering lower limbs exoskeletons: State-of-the-art. *Robotica*. 2018; 36(11): 1743–56.
4. Li WZ, Cao GZ, Zhu AB. Review on control strategies for lower limb rehabilitation exoskeletons. *IEEE Access*. 2021; 9: 40–60.
5. Liang X, Wang W, Hou Z, et al. Human-machine interaction control methods for rehabilitation robots. *Science China: Information Sciences*. 2018; 48(1): 23.
6. Kwon SH, Lee BS, Lee HJ, et al. Energy efficiency and patient satisfaction of gait with knee-ankle-foot orthosis and robot (ReWalk)-assisted gait in patients with spinal cord injury. *Annals of Rehabilitation Medicine*. 2020; 44(2): 31–41.
7. Zheng Y, Jing X, Li G. Application of human-machine intelligent collaboration in the field of medical rehabilitation robots. *Big Data Times*. 2018.
8. Fong J, Küçüktabak EB, Crocher V, et al. CANopen Robot Controller (CORC): An open software stack for human-robot interaction development. In: *Wearable Robotics: Challenges and Trends*. Springer Publishing; 2021. pp. 287–292.
9. Yan H, Wang H, Chen P, et al. Optimal design of upper limb rehabilitation robot with generalized shoulder joint. *Acta Armamentarii*. 2021; 42(11): 2491–2502.
10. Liu X, Yang M, Wang M, et al. Application of multi-position intelligent lower limb rehabilitation robot in rehabilitation training of stroke patients. *Biomedical Engineering and Clinical Medicine*. 2018; 22(3): 5.
11. Wang W, Song W, Qu S. Research and progress of upper limb rehabilitation robots in the rehabilitation of complications in stroke patients. *Massage & Rehabilitation Medicine*. 2018; 9(18): 3.
12. Luo S, Luo S, Lu Y, et al. Research on adaptive gait control method for walking-aid rehabilitation robots. *Machinery Design & Manufacture*. 2024; 6: 362–366.
13. Maranesi E, Riccardi GR, Di Donna V, et al. Effectiveness of intervention based on end-effector gait trainer in older patients with stroke: A systematic review. *Journal of the American Medical Directors Association*. 2020; 21(8): 36–44.
14. Ding H, Yang L, Yang Z, et al. Health status prediction of shearer driven by the fusion of digital twinning and deep learning. *China Mechanical Engineering*. 2020; 31 (7): 15-23.
15. Gao Y, Chen C, Zhang Y. Digital twin city: Mainstream mode of smart city construction [J]. *China Construction Informatization*. 2019; No.100 (21): 8-12.
16. Li J, Zhu L, Gou X. Kinematic analysis of lower limb rehabilitation exoskeleton mechanism based on human-machine closed chain. *Journal of Engineering Design*. 2019; 26 (1): 65-72,109.
17. Jiang S, Wang Z, Xia S, et al. Construction method of digital twin geometry model of aircraft flexible tooling [J]. *Aviation Manufacturing Technology*. 2022; 65(12): 86-91,111.
18. Jiang Y, Dong J. Application effect of lower limb rehabilitation robot training in rehabilitation treatment of patients with acute stroke. *Health World*. 2021; 6: 197.
19. Hua Y, Zhu M, Zhang Y. Current application status and development trend of pediatric rehabilitation robots. *Chinese Journal of Rehabilitation Theory and Practice*. 2018; 24(6): 4.
20. Chen W, Wang L, Zhang L, et al. Dynamic analysis and simulation of lower limb exoskeleton rehabilitation robot. *Machinery Design*. 2018; 35(4): 7.
21. Huang J, Yuan M, Wang S, et al. Structural design and simulation analysis of lower limb rehabilitation robot. *Mechanical & Electrical Engineering Magazine*. 2018; 35(2): 5.
22. Lv X, Yang C, Jiang F, et al. Passive training control of sit-and-lie lower limb rehabilitation robot. *Machinery Design & Manufacture*. 2019; 4: 244–247.
23. Sun Qi, Xie J. Effect of upper limb rehabilitation robot on upper limb dysfunction in stroke patients. *Chinese Journal of Physical Medicine and Rehabilitation*. 2023; 9: 45.
24. Li Y, Zeng Q, Huang G. Clinical application progress of upper limb rehabilitation robots in stroke. *Chinese Journal of Rehabilitation Theory and Practice*. 2020; 26(3): 5.
25. Shen Z, Zhang L, Su Y, et al. Autonomous adaptive control strategy based on ankle rehabilitation robot. *Chinese Journal of Medical Instrumentation/Zhongguo Yiliao Qixie Zazhi*. 2024; 48(4).